Energy Reports 8 (2022) 4196–4208

Contents lists available at ScienceDirect

Energy Reports

journal homepage: www.elsevier.com/locate/egyr

Research paper

Analysis of the thermodynamic performance of transcritical CO_2 power cycle configurations for low grade waste heat recovery

Veronika Wolf [a,*], Alexandre Bertrand [b], Stephan Leyer [a]

[a] University of Luxemburg, 2 Avenue de l'Universite, Esch-sur-Alzette, 4365, Luxembourg
[b] Luxemburg Institute of Science and Technology, 41 Rue de Brill, Belvaux, 4422, Luxemburg

ARTICLE INFO

Article history:
Received 19 October 2021
Received in revised form 18 February 2022
Accepted 7 March 2022
Available online xxxx

Keywords:
Waste heat recovery
Energy efficiency
Thermodynamic analysis
Supercritical CO_2
Rankine cycle
Cycle configuration

ABSTRACT

Organic Rankine cycles employing carbon dioxide (CO_2) for waste heat recovery became popular in the last years thanks to its excellent heat transfer characteristics and small environmental footprint. Low-grade waste heat (<240 °C) represents the major portion of excess heat globally, but it is hard to recover due to the small temperature gap of heat source and heat sink leading to a poor efficiency of the Rankine cycle. Therefore, numerous modifications of the power cycle layout were proposed by academia and industry — reheated expansion, recuperation and intercooled compression among them. This work compares ten cycle architectures for a defined waste heat source (60–100 °C) and heat sink (20 °C). Firstly, CO_2 cycle architectures from literature are examined with its original operational parameters. Secondly, the predefined low-grade heat source is implemented into the cycle. The cycles are assessed regarding efficiency, mass flow and pressure. Results show that for source temperatures higher than 80 °C, recuperation and reheated expansion enhance the cycle performance whereas intercooled compression negatively affects the efficiency. The conventional configuration operated most efficiently for temperatures until 80 °C. A road map of thermodynamic efficiencies of CO_2 cycle architectures for low-grade waste heat recovery up to 100 °C is delivered.

1. Introduction

With increasing global energy demand, efficient and economic use of heat grows more important. Especially since large amounts of waste heat is produced during the conversion of primary energy into secondary energy, e.g. electricity (Forman et al., 2016). The wasted energy can be classified into high (>480 °C or 753.15 K), medium (240–480 °C or 513.15–753.15 K) and low (<240 °C or 513.15 K) grade waste heat . The latter representing 63% of the total available waste heat (Forman et al., 2016). A problem for thermodynamic cycles associated with low grade waste heat is the narrow temperature difference between heat source and heat sink resulting in a big challenge for the cycle efficiency.

For the reuse of low and medium grade waste heat, the Organic Rankine Cycle (ORC) plays a predominant role. The technology employs organic C–H-based working fluids like hydrocarbons, halogens or siloxanes. These synthetically manufactured working fluids offer a reduced evaporation pressure which is beneficial for the power cycle operation (Alfani et al., 2021). Carbon dioxide (CO_2) as a working fluid is chemically more stable in comparison to conventional ORC refrigerants (Calm and Hourahan, 2001). It is also more environmentally friendly with an ozone depletion potential (ODP) of zero and a global warming potential (GDP) of 1 over 100 years (Sarkar, 2015).

Another characteristic of (CO_2) is the low critical temperature (30.98 °C or 304.04 K) and moderate critical pressure (73.77 bar) which can be achieved in the operating conditions of a power cycle (Li et al., 2014). Near the supercritical point, thermodynamic properties change rapidly with temperature, as shown in Fig. 1. These favourable properties lead to a high fluid density and hence to a great reduction in system size. Especially turbomachinery becomes very compact: Sandia research institute (Wright, 2012) reports a 30 times smaller turbine when operated with CO_2 instead of steam. However, elevated operation pressures are challenging for all sorts of system components. When CO_2 alternates between supercritical and subcritical pressures in a power cycle, the operation mode is then called transcritical. In the Rankine cycle, the working fluid undergoes a phase change and operates therefore transcritical while the Brayton cycle operates in gaseous state solely (Li et al., 2014).

Especially for the recovery of low grade waste heat, fluid properties play an important role. Every working fluid brings its own characteristics to deal with. The aforementioned positive aspects of the low critical temperature of (CO_2) can be limiting on the other hand: When using ambient air as heat sink within a

* Corresponding author.
E-mail address: veronika.wolf@uni.lu (V. Wolf).

https://doi.org/10.1016/j.egyr.2022.03.040

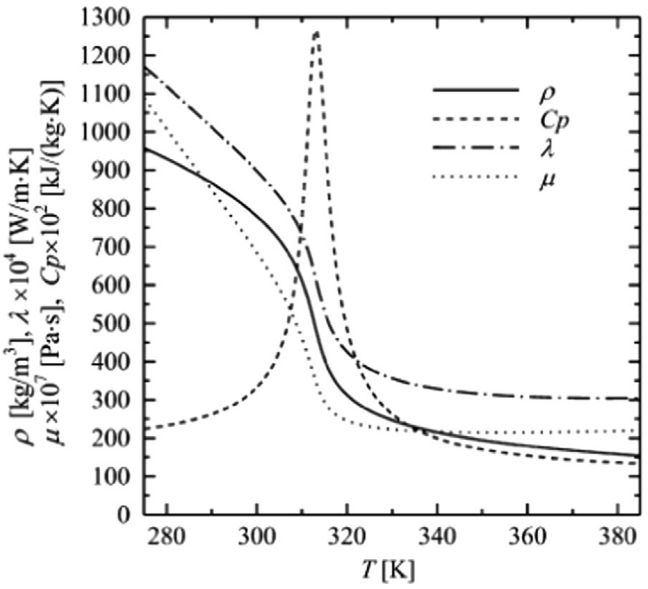

Fig. 1. Thermodynamic properties of CO_2 near the critical point (National Institute of Standards and Technology).

Rankine cycle, a cooling down below (31 °C) must be ensured in order to guarantee a reliable operation.

For other ORC refrigerants, the limiting fluid characteristic is the constant temperature evaporation. Because traditional organic working fluids have higher critical temperatures, the heat addition process happens in the two-phase-region whereas it happens in supercritical quasi-vapour state in a CO_2 power cycle. The difference in fluid behaviour can be seen in Fig. 2: the pinching problem within a heat exchanger occurs when a working fluid evaporates. When the working fluid is in quasi-vapour state, it can match the temperature profile of the waste heat stream more closely.

The CO_2 power cycle has been frequently researched for energy recovery in the high and medium temperature sector and very few investigations deal with the recovery of low temperatures although it shows great potential to recover low-grade waste heat because of good heat transfer characteristics. Accordingly, the study focuses on low-grade heat sources recovered by a CO_2 power cycle.

The basic power cycle configuration with a pump, heater, turbine and condenser has been widely studied. Ahmadi et al. (2017) use the basic cycle with solar energy as a heat source and LNG as a heat sink to increase the cycle efficiency by maximizing the temperature difference.

Habibollahzade et al. (2022) performed a multi-objective optimization of super- and transcritical CO_2 cycles for geothermal energy recovery. The simple transcritical CO_2 system achieved the highest energy and exergy efficiencies.

Xia et al. (2018) added an ejector to the basic power cycle configuration to solve the condensation problem of CO_2 under the higher temperature heat sink.

Meanwhile, many studies focus on the optimization of CO_2 power cycles by modifying the cycle architecture. Mirkhani et al. (2017) report an increased work output when adding reheated expansion to the basic cycle. In this configuration, the high pressure CO_2 is expanded to a medium pressure in a first stage, then reheated, and finally expanded to the lower cycle pressure.

Abid et al. (2020) found that a reheated expansion can improve the performance of a solar driven carbon dioxide power cycle by 11.6%. Siddiqui and Almitani (2020) proposed a power cycle layout with reheated expansion for improved heat recovery. Compared to the power cycle layout without reheat, the proposed variant improved the efficiency by 1.5%.

A power cycle with intercooled compression was studied by Olumayegun et al. (2016) for a gas turbine exhaust stream. When modifying a power cycle with intercooled compression, the CO_2 compression process is split into several smaller compression stages and the fluid is cooled in between these stages in order to lower the necessary compression energy. Nassar et al. (2014) developed an individual main compressor and recompression compressor for a CO_2 power plant. They also employed a recuperator within the cycle to transfer heat from the low pressure part of the cycle into the high pressure part. This reduces the cooling load significantly.

Garapati et al. (2020) examined a hybrid geothermal power system with recuperation. This arrangement generates up to 20% more electric power than in individual geothermal system.

Another cycle modification, which has been applied by numerous authors is the split flow configuration. In order to enhance the system performance, the working fluid is divided into sub streams, which are finally merged again at another point in the system. The split position can occur at different points of the system.

For a concentrated solar power application, Duniam and Veeraragavan (2019) investigated split flow before cooling cycle layout. After the split, one CO_2 stream is sent to the cooler while the second stream is recompressed directly without cooling. For an ambient air heat sink of 30° C, a system thermal efficiency of 46.2% is reported. Another work concerning concentrated solar power by Monjurul Ehsan et al. (2020) deals with a split flow before cooling and compression cycle configuration. In this variant, another cooler and compressor is added to the cycle. After passing the first section of cooling and compressing, the working fluid is split at an intermediate pressure. One part is cooled and compressed again, while the other part is compressed directly without further cooling. For compressor inlet temperatures above 50° C, the cycle variant showed a thermal efficiency of 45.5%.

A system configuration with split flow before heating was modelled by Walnum et al. (2013). A bottoming cycle for offshore oil and gas installations with a split of the CO_2 stream before the heater and a merge after the turbine was investigated. In this configuration, CO_2 showed 16% less power output than steam as working fluid.

Summarizing the findings in literature, there is an immense diversity of system layouts in power cycle architectures. Table 1 gives an overview of possible modifications. Applicable modifications in the system layout are not limited so that several modifications can be combined, for example split flow and recuperation as studied by Crespi et al. (2017). In addition, the number of recuperators can be increased, depending on the available thermal energy in the system. Where as a combination of cycle modification leads to a more complex system bigger in size.

Previous studies show that cycle modifications lead to changes in the cycle efficiency. All publications mentioned above are tailor made to the specific application. Especially the waste heat temperature and operational conditions strongly depend on the particular application. Consequently, the stated efficiencies of the findings above cannot be compared with each other as they rest upon different boundary conditions.

Available comparisons of CO_2 power cycle architectures are listed in Table 2: An analysis of four different cycle configurations has been performed by Pham et al. (2015) for nuclear reactors (a small modular reactor and a sodium-cooled fast reactor). For turbine inlet temperatures until 850 °C, a cycle optimization in terms of exergy was performed. Among recompression cycle, reheated recompression cycle, intercooled recompression cycle and

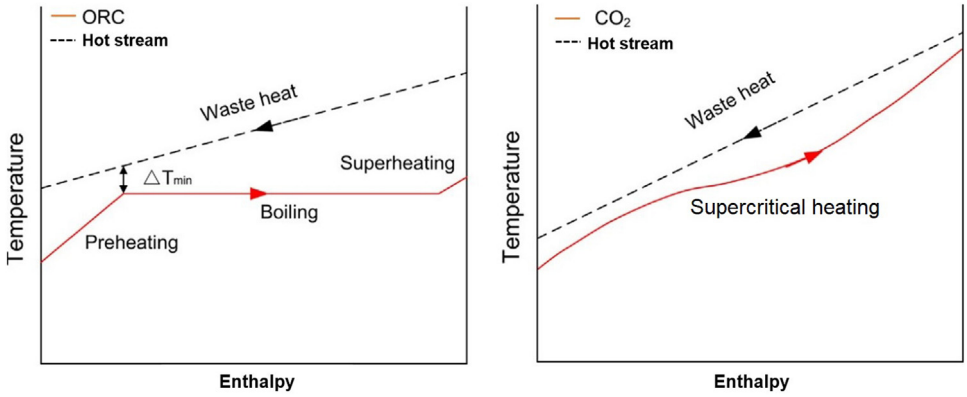

Fig. 2. Heat addition process of traditional ORC compared with CO_2 (Wang and Dai, 2016).

Table 1
Types of power cycle modifications.

Single flow modifications		Split flow modifications	
SR	Single Recuperation	SFC	Split flow before cooling/compression
DR	Double Recuperation	SFH	Split flow before heating
RE	Reheated expansion	SFE	Split flow before expansion
IC	Intercooled compression	SFHE	Split flow before heating and expansion

Table 2
Available comparisons of CO_2 power cycle architectures.

Study	Name of cycle architecture	Modifications	Temperature range
Pham et al. (2015)	Recompression cycle	SFC,DR	250–850 °C
	Reheated recompression cycle	SFC, DR, RE	
	Intercooled recompression cycle	SFC, DR, IC, RE	
	Partial-cooling cycle	SFC, DR, IC	
Alfani et al. (2021)	Simple recuperative cycle	SR	550 °C
	Recompressed recuperative cycle	SFC, DR	
	Simple recuperative cycle with recuperator bypass	SFH, SR	
	Recompressed recuperative cycle with high temperature recuperator bypass	SFC, SFH, DR	
	Turbine split flow cycle	SFHE, DR	
Marchionni et al. (2018)	Single Regenerated	SR	600 °C
	Re-Heating	SR, RE	
	Re-Compression	SFC, DR	
	Re-Compression Re-Heating	SFC, DR, RE	
	Pre-Heating	SFH, SR	
	Pre-Heating Split-Expansion	SFH, SFHE, DR	
	Split-Heating Split-Expansion	SFHE, DR	
	Pre-Heating Pre-Compression	SFH, SR, IC	
Binotti et al. (2017)	Recompression cycle	SFC, DR	750 °C
	Partial cooling cycle	SFC, IC, DR	
	Recompression main compressor intercooling	SFC, DR	

partial-cooling cycle, the power cycle that achieved the highest efficiency was the recompression cycle with double recuperation and a split flow before compression.

Alfani et al. (2021) published a design optimization for sCO_2 power plants with five different configurations (single recuperative cycle, recompressed recuperative cycle, simple recuperative cycle with recuperator bypass and recompressed recuperative cycle with high temperature recuperator bypass). The authors used a high grade heat source of 550 °C and concluded that the simple recuperative cycle with recuperator bypass is the most promising configuration. The cycle configuration uses two heat exchangers to extract energy from the heat source as well as a recuperator.

An techno-economic assessment of various Joule–Brayton cycle architectures for high-grade heat sources (650 °C) was conducted by Marchionni et al. (2018). Power cycle configurations were taken from concentrated solar power and nuclear applications. An exergy analysis was followed by a analysis of several economic indicators like specific cost per unit power and levelized cost of electricity. The results showed that the most complex sCO_2 cycle configurations lead to higher overall efficiency but also have higher investment costs.

A further analysis of sCO_2 cycles for power generation in CSP solar tower plants has been carried out by Binotti et al. (2017), where three different power cycle were optimized for turbine inlet temperatures until 800 °C. The tested recompression cycle, partial cooling cycle and recompression main compressor intercooling cycle employ each several recuperators and compressor steps. The cycle configuration with split flow before cooling and intercooled compression, called recompression with main compressor intercooling, showed the highest solar to electric efficiency.

These aforementioned studies compare few CO_2 power cycle architectures using high temperature heat sources. The cycle assessments in literature contain Brayton cycles with no condensation of the working fluid due to their high target temperature

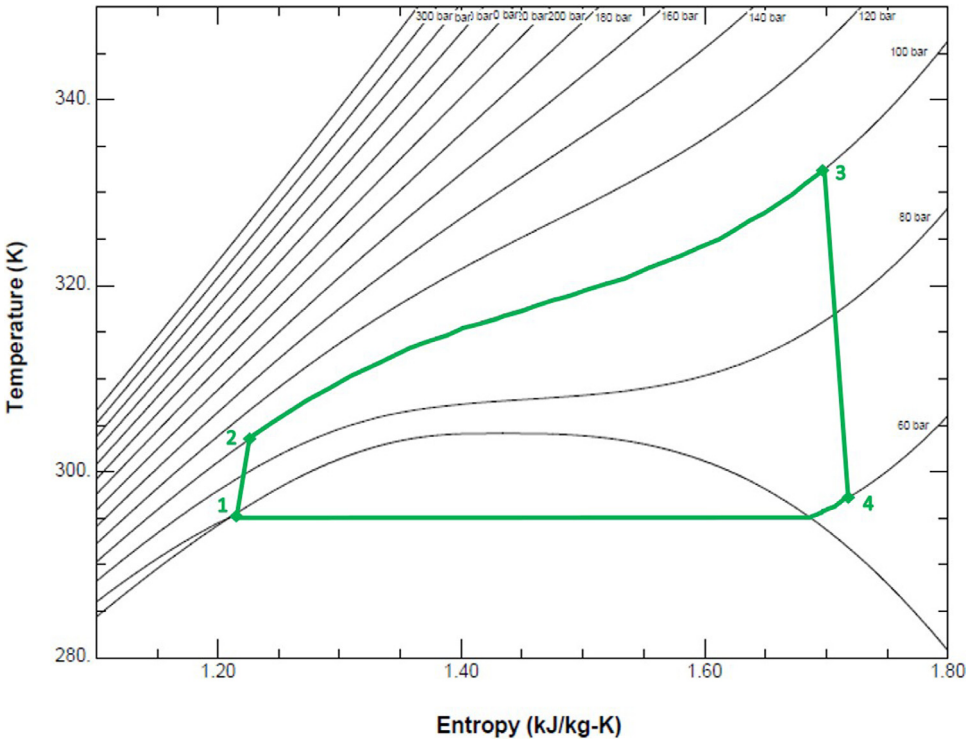

Fig. 3. TS diagram of basic CO_2 power cycle configuration.

range. Thus, the findings are not suitable for low-grade waste heat sources.

Despite the abundance of low temperature waste heat worldwide, no comparative study on suitable power cycle configurations for power generation exists on this field. There is a clear gap in currently available research studies dealing with low temperature heat source power cycles.

This work aims at filling this gap of knowledge and provides a systematic assessment and comparison of ten different cycle architectures for a waste heat source temperature range between 333.15 to 373.15 K. A thermodynamic assessment is carried out and a performance optimization is conducted as function of the system pressure ratio, mass flow and specific work output.

2. Methods

Uniform operational conditions for the cycle comparison are defined as follow: The waste heat source is air, which provides temperatures between 333.15–373.15 K at a mass flow rate of 100 kg/s. The heat sink is ambient air at a temperature of 293.15 K.

According to the low temperature heat source and sink, the CO_2 alternates between subcritical and supercritical pressure, representing a Rankine cycle. The mass flow of the heat sink is adjusted to ensure a full condensation of the working fluid. Isentropic efficiencies of turbo machinery (pump and turbine) are set to be 80%. The effectiveness of the heat exchanger is 95% (Meggitt PLC).

The different power cycle configurations are implemented in EBSILON® Professional (Steag System Technologies), a commercial simulation software for energy and mass flow balancing of power plants. It uses REFPROP database (National Institute of Standards and Technology) for fluid properties, which employs the Span–Wagner equation of state for CO_2 (Span and Wagner, 1996). EBSILON uses the specified values of the system components to set up a non-linear system of equations, which is solved iteratively using a Newton-like linearization and a matrix solution.

Firstly, the power cycle architectures with their original operational conditions as stated in literature were modelled in EBSILON. Only when the setup and results matched with the publication, the previously specified uniform operational conditions were applied. Each power cycle architecture is compared in terms of the thermodynamic efficiency η_{th}:

$$\eta_{th} = \frac{\dot{W}_{net}}{\dot{Q}_{in}} \tag{1}$$

$\dot{Q}_{in}$ is the waste source heat flux absorbed by the heat exchanger(s) and $\dot{W}_{net}$t is the net power output:

$$\dot{W}_{net} = \dot{W}_{Turbine} - \dot{W}_{Pump} \tag{2}$$

In Eq. (2), the turbine output power $\dot{W}_{Turbine}$ and pump input power $\dot{W}_{Pump}$ are calculated via the following formulas:

$$\dot{W}_{Pump} = \dot{m}_{CO_2} * \frac{(h_{2,is} - h_1)}{\eta_{Pump}} \tag{3}$$

$$\dot{W}_{Turbine} = \dot{m}_{CO_2} * (h_3 - h_{4,is}) * \eta_{Turbine} \tag{4}$$

In Eqs. (3) and (4), the numbers in subscript of the specific enthalpies h represent the state points in the system as shown in Fig. 3. As it can be observed in the compression process from state point 1 to 2, the CO_2 changes its state from liquid to quasi-vapour. This so-called superheating is unique for the transcritical operation of a power cycle.

The equations for heat addition and removal are the following:

$$\dot{Q}_{in} = \dot{m}_{CO_2} * (h_3 - h_2) \tag{5}$$

$$\dot{Q}_{out} = \dot{m}_{CO_2} * (h_4 - h_1) \tag{6}$$

The theoretic Carnot efficiency η_{Carnot} is calculated with the temperatures of the heat sink (here: ambient air) T_{cold} and the

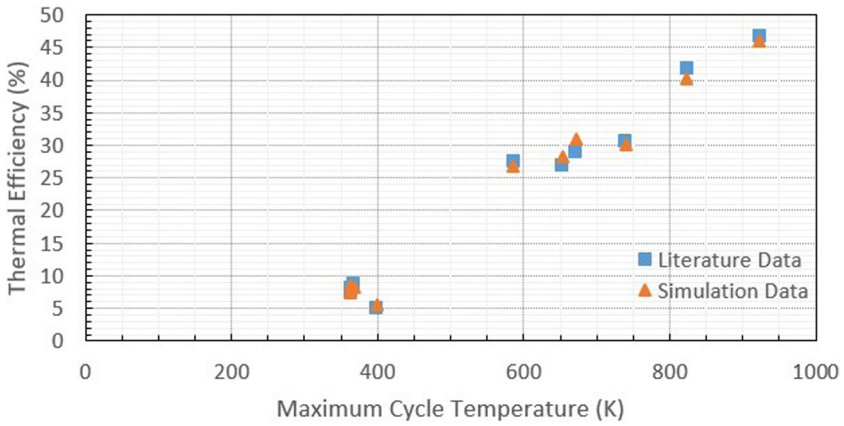

Fig. 4. Verification of simulation data with literature data.

heat source (waste heat temperature) T_{hot}:

$$\eta_{Carnot} = 1 - \frac{T_{cold}}{T_{hot}} \tag{7}$$

With Eq. (7), an idealistic Carnot efficiency of 12.0% to 21.4% can be reached for T_{cold} being 293.15 K and T_{hot} equal to 333.15 K and 373.15 K, respectively.

With every iteration in waste heat temperature, the thermodynamic efficiency is optimized by pressure ratio:

$$r_P = \frac{P_{High}}{P_{Low}} \tag{8}$$

In Eq. (8), P_{High} denotes the high pressure part and P_{Low} denotes the low pressure part of the power cycle. With more compression and expansion stages, the highest and lowest pressures are taken in this equation.

The validation process was framed in a way that the original cycle layout from publication was modelled with its stated operational parameters. Fig. 4 shows a comparison of data taken from literature and simulation results performed within the current study with the same input parameters. Efficiencies show a maximum deviation of 1.99 percent. After reaching accordance of the obtained results with published ones, the previously defined uniform parameters for the cycle assessment were applied to the power cycle layouts. The outcome of the comparative study with unified conditions is shown in the next chapter.

3. Results

Fig. 5 displays the basic cycle configuration and Fig. 6 the corresponding efficiency in comparison to the Carnot efficiency. The difference of the basic and Carnot cycle efficiency are diverging with increasing heat source temperature. It can be seen that the gain of efficiency with rising heat source temperature is rather flat in comparison to the ideally reachable efficiency. The efficiencies shown in Fig. 6 are based on an optimization of the pressure ratio to obtain a maximum net power output. Because the system components are modelled based on the enthalpy of the working fluid at this point (Eqs. (1)–(8)), the enthalpy within a system component is different with varying pressure. Thus, the resulting net power output also changes and an optimum value can be found.

By plotting the cycle pressure ratio on thermal efficiency, the optimization of cycle pressure ratio is illustrated in Fig. 7 for a waste heat source temperatures from 333.15 K to 373.15 K. It should be emphasized that the pump and turbine efficiencies were assumed fixed in different pressure ratios to show the potential thermodynamic behaviour of the system with ideal

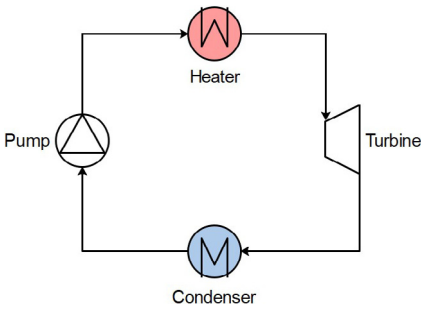

Fig. 5. Basic cycle configuration.

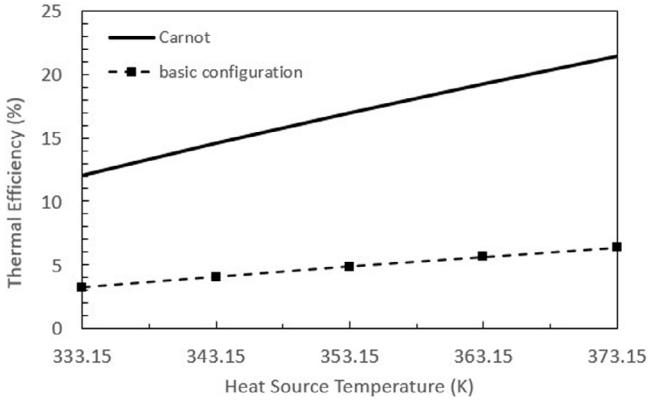

Fig. 6. Basic cycle and Carnot thermal efficiency.

components. One can see that it exists a maximum (optimum) pressure ratio in the parabolic shaped efficiency curve. If parameters like heat source temperature or system configurations are changed, the amplitude of the curve changes as well. Whereas for an increase of waste heat temperature, a proportional rising amplitude towards higher efficiency can be observed and the maximum is shifted to the right towards a higher pressure ratio. A change in system configuration causes the curve to either augment or descent, depending on the specific modification. It is observed that this shape is not unique for this basic system configuration example, but for all modelled configurations.

The subsequent cycle configurations will be compared to the basic cycle configuration, as it serves as initial point for modifications. Thus, only with this cycle configuration, a comparison is legitimate and it can be analysed, whether a modification in the cycle architecture leads to a higher efficiency.

Table 3
Results of performance comparison of single flow cycle architectures.

Cycle variant	Heat source temperature (K)	Turbine inlet pressure (bar)	Condensation pressure (bar)	Net power output (kW)	Thermal efficiency (%)
Basic cycle	333.15	100	65	78.3	3.21
	343.15	108	65	135.5	4.04
	353.15	118	65	200.1	4.85
	363.15	128	65	277.0	5.63
	373.15	138	65	365.3	6.38
IC	333.15	100	65	59.9	2.35
	343.15	106	65	86.6	3.26
	353.15	116	65	121.1	4.16
	363.15	126	65	153.1	4.99
	373.15	135	65	189.0	5.79
IC + RE	333.15				
	343.15	104	65	117.2	3.73
	353.15	112	65	156.1	4.76
	363.15	122	65	196.6	5.61
	373.15	134	65	238.2	6.50
RE	333.15				
	343.15	104	65	132.5	4.25
	353.15	114	65	171.4	5.14
	363.15	124	65	213.6	5.99
	373.15	137	65	358.3	6.68

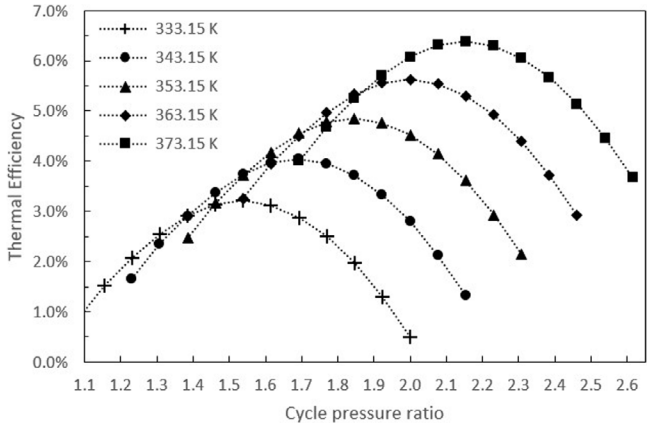

Fig. 7. Cycle efficiency of basic cycle configuration with different heat source temperatures in terms of pressure ratio.

3.1. Single flow configurations and their efficiencies

The modification of intercooled compression possesses two pumps and two coolers as shown in Fig. 8a.

Here, two steps of compression are displayed as simulated in EBSILON. A comparison between the efficiencies of the basic cycle and intercooled compression cycle is shown in Fig. 8d: One can see that intercooled compression affects the cycle efficiency negatively by one percentage point. Towards higher temperatures, the efficiency curve gets closer to the basic cycle efficiency and thus, there exists a point from which the addition of intercooled compression enhances the efficiency. Within the modelling process, it was calculated that this break-even point of the two efficiency lines is at 713.15 K.

The principle of reheated expansion (RE) is the separation of the expansion process into several steps (Fig. 8b), derived from the idea to achieve an isothermal like expansion of the fluid. A two-step expansion is modelled in this work. Generally, more steps are possible. In the first expansion step, the working fluid is expanded to an intermediate pressure between high-pressure side and low-pressure side. Then, it follows another heat input and an expansion to the low cycle pressure.

Fig. 8d shows the resulting thermal efficiencies with respect to different heat source temperatures. Note that for the reheated expansion configuration, an implementation at a waste heat source temperature as low as 333.15 K was not possible: At low source temperatures, the maximum possible cycle pressure is also lower. Thus, the cycle pressure ratio is small, as shown in Table 3. The solver did not succeed to iterate for an intermediate pressure, at which the fluid could be expanded a second time without condensation within the second turbine. The solver converged at a source temperature of 343.15 K with a cycle pressure of 104 bar. At this point, reheated expansion improves the efficiency by 0.3 percentage points. The efficiency plots are diverging towards higher source temperatures with the reheated expansion configuration having a steeper rise in efficiency than the basic system layout. At a source temperature of 373.15 K, reheated expansion contributes to a 0.7 percentage points higher cycle efficiency. Thus, reheated expansion becomes more significant with rising waste heat temperatures.

Comparing system pressures from Table 3, it can be noticed that the turbine inlet pressure of the RE configuration is slightly lower than the one obtained for the basic cycle. Yet, a higher efficiency is reached with reheated expansion.

The thermodynamic analysis further showed that the intermediate pressure between the expansion stages is crucial for the cycle performance.

Between the high pressure part and the low pressure part of the power cycle, there is a certain energy content that can be extracted by the turbines. Before the first expansion stage, the working fluid has the highest energy content. After the first expansion, there is a reduced pressure, which is left for the second expansion stage.

Best results were obtained with an intermediate pressure closer to the high pressure of the cycle with a pressure ratio of high pressure to intermediate pressure of 1.13.

The power cycle configuration shown in Fig. 8c combines the modifications of intercooled compression and reheated expansion. Its efficiency plot (Fig. 8d) is relatively close to the efficiency of the basic cycle. This results from the combination of reheated expansion, which enhances the cycle efficiency and intercooled compression, which decreases the cycle efficiency for low temperatures. In comparison to the basic configuration, this combination of modifications resulted in a slightly lower turbine inlet pressure (Table 3). It is found that a source temperature

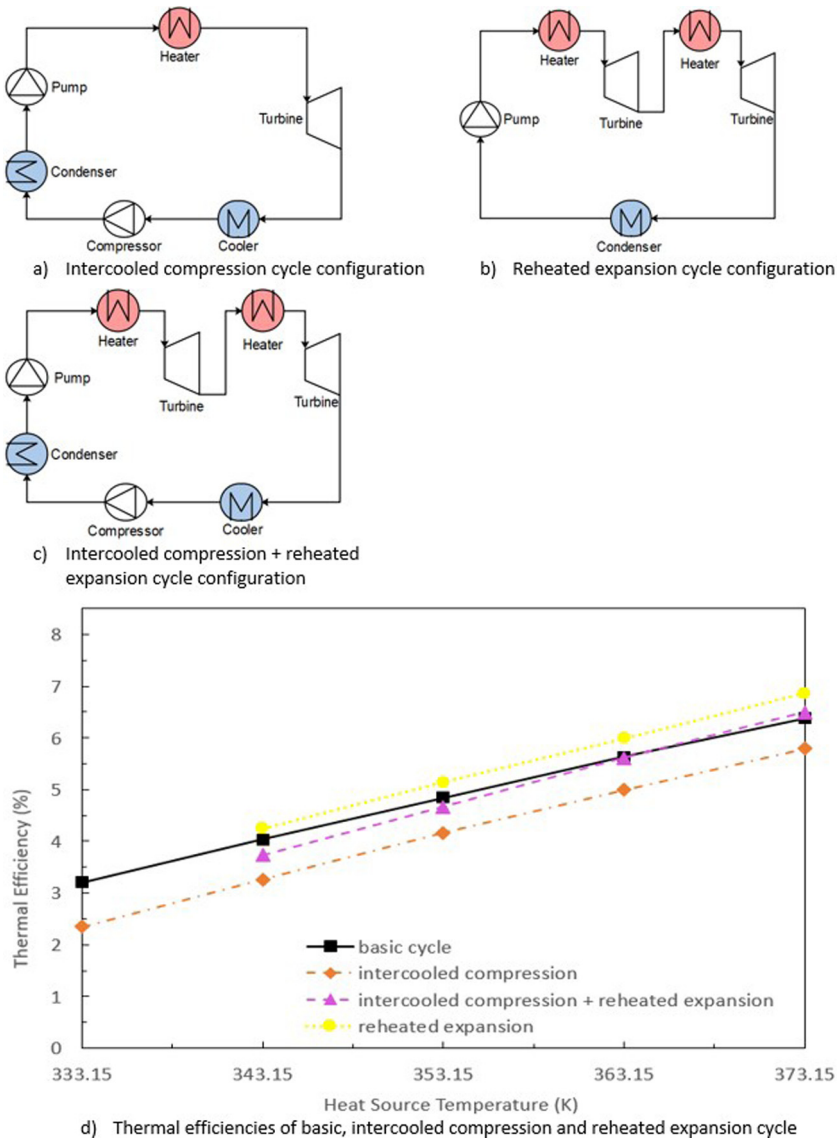

Fig. 8. Intercooled compression and reheated expansion cycle configurations and efficiencies.

of 333.15 K is too low for this configuration to be implemented as the small pressure ratio impedes the addition of reheated expansion. At 343.15 K, the basic configuration performs better by 0.31 percentage points. At 363.15 K, there is a turning point where this combination of modifications outperforms the basic configuration. There is a trend towards a greater efficiency gain in higher waste heat temperatures and the difference in thermal efficiency accounts for 0.12 percentage points at a waste heat temperature of 373.15 K.

3.2. Recuperative single flow configurations and their efficiencies

Fig. 9a shows a system configuration that employs one recuperator (SR) to transfer heat from the expanded fluid to preheat the compressed fluid prior to the heater. The benefit from adding a recuperation step is the reduction of discharged heat to the heat sink. Consequently, the thermal energy at turbine exit does not have to be removed by the condenser, but can be transferred to the high pressure side of the power cycle. Fig. 9d displays the resulting efficiency with regards to the waste heat source temperature. For temperatures as low was 333.15 K and 343.15 K, an additional recuperator step degrades the cycle efficiency by 0.17 and 0.09 percentage points, respectively. In order for a recuperator to transfer thermal energy from the low pressure side of the cycle to the high pressure side, the temperature of the working fluid after the turbine must be higher than after compression. For waste heat temperatures of 333.15 K and 343.15 K, the temperature difference between turbine exit and pump exit is narrow that no thermal energy can be transferred. The increasing heat source temperature also increases the amount of transferable heat within the recuperator leading to an augmentation of the thermal efficiency by one percentage point for each step of 10 K. It is interesting to note that the addition of a recuperator to the basic cycle decreased the maximum turbine inlet pressure by 17.1 percent, as can be seen in Table 4. This means that the SR configuration reaches higher efficiencies with a lower pressure ratio. The lower turbine inlet pressure benefits the thermal efficiency by decreasing the compression energy. As a consequence, the net power output rises.

A grouping of intercooled compression and recuperation (Fig. 9b) decreases the efficiency for source temperatures of 343.15 K (Fig. 9e) by 1 percentage point. The efficiency line approaches the basic cycle efficiency line with rising source temperatures and outperforms it at 391.6 K. Table 4 shows that

Table 4
Results of performance comparison of recuperative single flow cycle architectures.

Cycle variant	Heat source temperature (K)	Turbine inlet pressure (bar)	Condensation pressure (bar)	Net power output (kW)	Thermal efficiency (%)
SR	333.15	91	65	80.9	3.04
	343.15	98	65	132.9	3.95
	353.15	105	65	198.1	4.86
	363.15	111	65	274.9	5.77
	373.15	120	65	366.4	6.67
SR + IC	333.15				
	343.15	94	65	93.1	3.04
	353.15	104	65	126.7	3.99
	363.15	109	65	162.1	4.95
	373.15	116	65	194.7	5.91
SR + IC + RE	333.15				
	343.15	97	65	73.9	4.18
	353.15	109	65	99.3	5.37
	363.15	119	65	125.6	6.52
	373.15	129	65	153.1	7.61
SR + RE	333.15	88	65	81.5	3.34
	343.15	102	65	121.0	4.62
	353.15	110	65	159.0	5.68
	363.15	118	65	198.1	6.73
	373.15	126	65	237.1	7.77

the SR + IC variant results in very low turbine inlet pressures. At a heat source temperature of 373.15 K, the corresponding maximum cycle pressure is 116 bar. This is the lowest pressure amount all power cycle architectures modelled. The reason why a combination of the two modifications results in a very low cycle efficiency is that each modification targets the thermal energy of the working fluid in gaseous state, which accounts for a very small fraction. This small amount of enthalpy is distributed to both cycle modifications.

Already from very low waste heat source temperatures, the combination of recuperation and reheated expansion (Fig. 9c) outperforms the basic configuration. While for 333.15 K, the difference between their efficiencies is rather small (0.1 percentage points), the difference in efficiency grows rapidly with increasing heat source temperature (Fig. 9e). At a waste heat source temperature of 373.15 K, the difference in efficiency already represents 1.4 percentage points.

It is worth noting that the high thermal efficiency is achieved with a turbine inlet pressure 8.7 percentage points less than when compared to the basic cycle configuration as shown in Table 4. In fact, the SR + RE combination offers the second highest efficiency of 7.77 percent with the second lowest turbine inlet pressure within this comparison.

Observing from Fig. 9e, the combination of recuperation, intercooled compression and reheated expansion (Fig. 9d) is one of the most complex cycle architectures in this study. The cycle configuration was modelled with nine components, where intercooled compression and reheated expansion have two stages each.

From a source temperature greater than 343.15 K, the SR + IC + RE combination shows a steep rise in efficiency with increasing waste heat source, which is steeper than the slope of SR + RE combination. In fact, this cycle architecture shows the steepest slope between all cycles compared in this work. At a waste heat temperature of 373.15 K, the difference in efficiency amounts to 1.22 percentage points to the basic cycle.

However, for the investigated range of waste heat, numerical results from Table 4 show that this system layout is less attractive than the combination of SR + RE due to the negative influence of intercooled compression for low temperature waste heat, which accounts for a 0.6 percentage point efficiency reduction. Both configurations resulted in similar turbine inlet pressures, however, the net power output of SR + RE combination is preferably higher than SR + IC + RE variant.

3.3. Split flow configurations and their efficiencies

Among the split flow cycle configurations introduced in Section 1, the cycle variants applicable for low grade waste heat recovery are discussed in this section. By their nature, split flow cycles consist of a great number of components, e.g. several heat exchangers, turbines and/or compressors. Thus, the system becomes complex very easily and does not apply to low temperature heat sources anymore. The remaining cycle configurations have been limited to one internal heat exchanger.

The presented system layout in Fig. 10a is a split flow before heating (SFH) configuration. The CO_2 mass flow is split into two streams after the pump and merges them before the second stage of heat addition. The stream indicated with green colour is preheated by the low temperature waste heat source while the stream indicated with orange colour is preheated by the internal recuperator.

Fig. 10c shows the performance for split flow configurations. For the configuration with split flow before heating, a modelling for a waste heat source temperature of 333.15 K did not converge because of the recuperator step: the available heat after the expansion process is not enough to employ a heat exchanger. From source temperatures greater than 343.15 K, it can be noticed that this cycle architecture outperforms the basic configuration by 0.73 percentage point increasing to 1.78 percentage points at 373.15 K.

Detailed numerical results are given in Table 5. It is worth stating that this cycle architecture produced the highest efficiencies throughout the cycle comparison: 8.16 percent. With a maximum pressure of 147 bar, the SR + SFH configuration achieved a 6.5 percentage points higher turbine inlet pressure than the basic cycle configuration. This represents the highest cycle pressure of all compared system variants.

The strong performance arises from the allocation of two heat exchangers for the heat addition process. Thus, the heat source can be exploited more efficiently than in other configurations. The working fluid is split before the first heat addition, where one stream is directed to the recuperator and the other stream is lead to the first external heat exchanger. The fluid streams are united before passing a second external heat exchanger. It is observed that the cycle efficiency is sensitive to the ratio between the CO_2 split fractions. For low grade waste heat sources, the internal energy transfer is lower than the enthalpy rise that can be

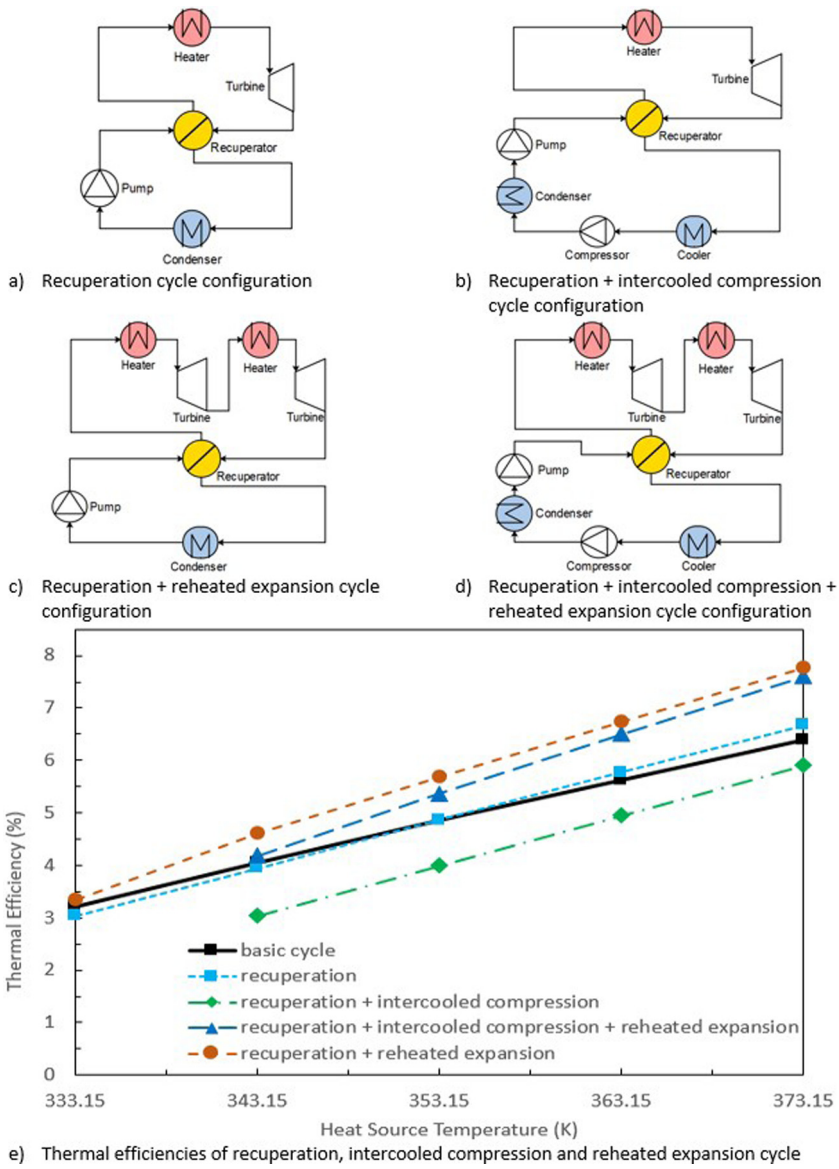

Fig. 9. Recuperation with modifications configurations and efficiencies.

Table 5
Results of performance comparison of split flow cycle architectures.

Cycle variant	Heat source temperature (K)	Turbine inlet pressure (bar)	Condensation pressure (bar)	Net power output (kW)	Thermal efficiency (%)
SR + SFH	333.15				
	343.15	99	65	151.7	4.77
	353.15	113	65	197.8	5.99
	363.15	137	65	269.7	7.24
	373.15	147	65	351.1	8.16
SR + SFHE	333.15				
	343.15	98	65	131.4	3.91
	353.15	104	65	195.6	4.83
	363.15	112	65	273.5	5.74
	373.15	120	65	362.8	6.64

obtained from the external heat source. Thus, the optimum split ratio between external and internal heat addition was computed to be 0.68.

The split flow before heating and expansion (SFHE) configuration (Fig. 10b) separates the CO_2 mass flow after the pump and merges it after the expansion process.

While the CO_2 stream indicated in green colour has one heat addition, the fluid stream indicated in orange colour is first preheated by the internal recuperator and secondly heated by the external heat source. This leads to a higher turbine inlet temperature. In the resulting efficiencies (Fig. 10c), the recuperator step prohibited an implementation of this architecture for a waste heat source of 333.15 K. However, a steeper slope of the thermal

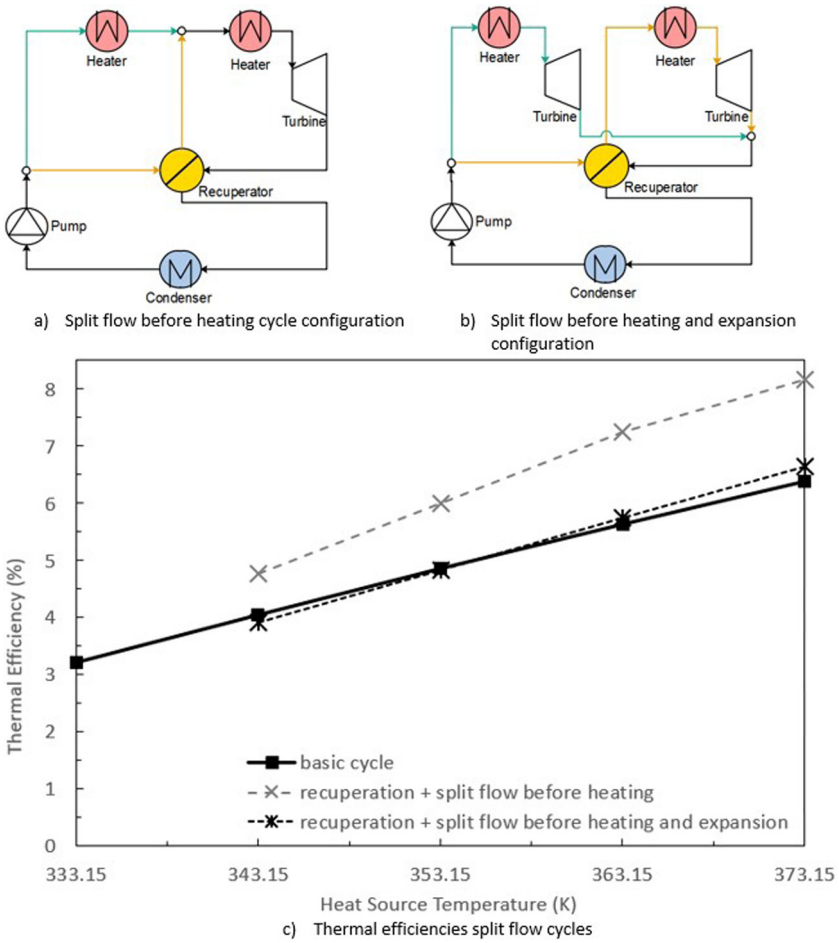

Fig. 10. Split flow configurations and efficiencies. (For interpretation of the references to colour in this figure legend, the reader is referred to the web version of this article.)

efficiency can be observed in comparison to the basic power cycle configuration having an intersecting point at a heat source temperature of 354.9 K.

At a heat source temperature of 373.15 K, the SFHE variant outperforms the basic variant by 0.26 percentage points. From Table 5, it can be noticed that the SFHE cycle delivers a similar net power output than the basic cycle with 18 bars less turbine inlet pressure. With turbine inlet pressures from 98–120 bar, these cycle pressures are among the lowest values of the compared architectures.

The heat addition process in this configuration is different from the split flow before heating configuration: the separated fluid streams are heated unevenly. While the first stream passes one external heat exchanger, the second fluid stream passes the recuperator and an external heat exchanger. However, the enthalpy difference is not significant because of the small amount of heat transferred by the recuperator. As the waste heat temperature increases, the recuperator contributes a bigger share towards the preheating of the second fluid stream. This can be observed in the shift of split ratio. For waste heat temperatures of 333.15 K, the optimum split is 0.82, the majority of fluid stream passing only one external heat exchanger. At a waste heat temperature of 373.15 K, the split ratio has augmented to 0.31, only a minor share passing one external heat exchanger and the majority of fluid stream passing the recuperator first.

3.4. Global comparison of cycle configurations

Fig. 11 shows the result from previous sections consolidated in one plot. It can be seen that the basic power cycle without any modifications is suited almost midway among the resulting efficiencies. A maximum difference of 1.4 percentage points is noticed at a heat source temperature of 373.15 K between the basic cycle and the system with split flow before heating (SR + SFH). This is because of the second heat exchanger for extraction of the waste heat source.

Also the recuperation and reheated expansion (SR + RE) variant delivers very good results in terms of thermodynamic first law efficiency, it ranks second highest among all cycle architectures. Similar to the SR + SFH variant, the SR + RE cycle employs two heat exchangers for heat source extraction. Especially for low grade waste heat sources, it seems crucial to effectively use the thermal energy provided.

All plots of system architectures with a recuperator show a steeper rise in efficiency than systems without recuperation. The steepest slope among all cycle architectures has the system configuration that contains the most modifications: recuperation, intercooled compression and reheated expansion.

System layouts with intercooled compression have a lower thermal efficiency than the basic cycle in the investigated temperature regime.

The benefit of intercooled compression is in general, that a gas requires less compression work when its specific energy content is lower. For the case of low-grade heat sources, the working fluid within the power cycle alternates between gaseous and liquid state. However, a major share of the low pressure part of the cycle is in liquid state. Thus, the possible range in which the intercooled compression can take place is narrow and the benefit of intercooled compression cannot be exploited at low waste heat

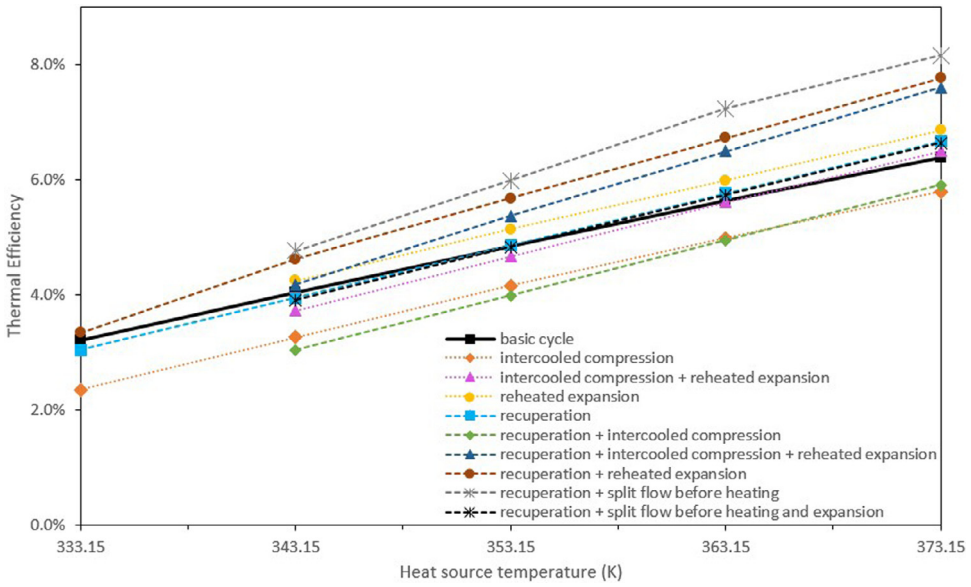

Fig. 11. Efficiencies of cycle architectures with respect to heat source temperature.

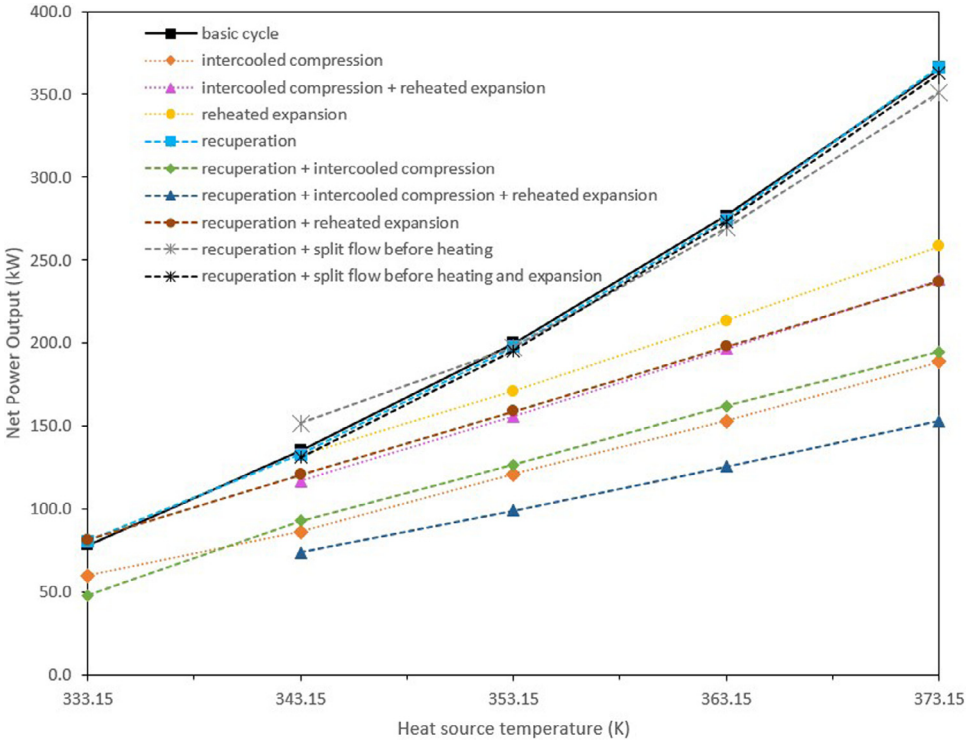

Fig. 12. Net power output of cycle architectures with respect to heat source temperature.

temperatures less than 333.15 K. Unlike the Rankine cycle, the Brayton cycle operates the low pressure part in gaseous phase and can therefore benefit from intercooled compression to a great extent.

The plots of basic cycle, recuperation and intercooled compression with reheated expansion are situated very dense, meaning that there is an minor change in efficiency for the given temperature range.

The main message of Fig. 11 is that the applied cycle modifications affect the thermal efficiency in a minor percentage range for very low heat source temperatures leading to a dominant role of the conventional power cycle.

Particularly for low grade heat sources, the thermal efficiency is not the only indicator of importance. Often, low temperature heat sources have high quantities of heat and low quality. Hence, a second indicator for the operation of a power cycle is the net power output. For all investigated cycle configurations, the corresponding net power outputs are mapped in Fig. 12. It is worth mentioning that the highest net power outputs could be achieved by the basic configuration, recuperation configuration as well as both split flow configurations. This finding reinforces the importance of the basic power cycle architecture: for a given amount of waste heat, it produces the most electrical energy with the least number of system components. Even if the most complex cycle architectures were among the most efficient in Fig. 11,

they produced the least net power output. The discrepancy in between the plots in Figs. 12 and 11 can be explained by their waste heat utilization rate. More complex cycles focus on a better utilization of thermal energy within the power cycle, being therefore more efficient. As a consequence, top performance requires less mass flow rate than in simple cycle configurations. For high temperature waste heat sources, this is a benefit. However, for the given low temperatures in this study, the lower mass flow rate has a direct impact on the net power output.

4. Conclusions

Increasing the worldwide energy efficiency is necessary for energy sustainability in future. Large parts of energy remain unused in the form of the waste heat. Especially low grade waste heat is hard to recover due to the small temperature difference between heat source and heat sink. The CO_2 Rankine cycle is an option to recover waste heat and various cycle configurations have been proposed. Current literature lacks cycle comparisons for low grade waste heat sources. This work provides a thermodynamic assessment of ten different cycle variants for a low temperature waste heat source under unified operational parameters. The obtained efficiencies range between 1.68 and 7.77 percentage points, for a waste heat temperature regime up to 373.15 K.

The comparison revealed that the basic configuration performs best at heat source temperatures as low as 333.15 to 353.15 K. For this sector, the small temperature range between heat source and heat sink limits the amount of applicable cycle modifications. Cycle modifications like recuperation start to be beneficial for temperatures above 353.15 K. Recuperation also contributes to a steeper gradient of the efficiency and results in diverging slopes of recuperative and basic system. Split flow before heating performed best within this comparative study above heat source temperatures of 353.15 K with a system efficiency of 8.16 percent, 1.4 percentage points higher than the basic system performance. The modification with reheated expansion proved to enhance the thermal efficiency by 0.7 percentage points, which is small for low-grade waste heat. For rising waste heat temperatures, the benefit becomes greater. Intercooled compression decreased the thermal efficiency constantly by approximately 1 percentage point due to the limited gaseous state in the low pressure part of the power cycle. For waste heat temperatures greater than 465.15 K, intercooled compression enhances the system performance. Throughout the given temperature range, the basic cycle architecture scored the highest net power output leading to a reinforcement of its dominant role for low grade waste heat recovery.

The higher efficiency of more complex cycle architectures is based on a better utilization of thermal energy within the power cycle. For low temperature waste heat, this results in less waste heat utilization and hence a lower net power output.

In conclusion, the challenge to recover waste heat from sources with temperatures lower than 373.15 K can be addressed by CO_2 cycles. However, the small operation temperature range excludes several cycle architectures involving measures that were found to be beneficial for higher operation temperature. Within this study, cycle modifications lead to a minor change in efficiency. For the design of such systems, the basic cycle configuration is recommended especially for source temperatures lower than 353.15 K. For source temperatures higher than 353.15 K measures like recuperation can be considered. However, the efficiency gain needs to be compared to the increased complexity of the cycle and the related investment cost.

CRediT authorship contribution statement

Veronika Wolf: Conceptualization, Methodology, Software, Validation, Investigation, Writing – original draft, Visualization, Funding acquisition. **Alexandre Bertrand:** Methodology, Formal analysis, Writing – review & editing. **Stephan Leyer:** Methodology, Validation, Writing – review & editing, Supervision, Project administration, Funding acquisition.

Declaration of competing interest

The authors declare that they have no known competing financial interests or personal relationships that could have appeared to influence the work reported in this paper.

Acknowledgements

The authors would like to thank to the Luxembourg National Research Fund (FNR), Luxembourg for the financial support. This project has been conducted under the grant AFR 12541056.

References

Abid, M., Khan, M.S., Ratlamwala, T.A.H., 2020. Comparative energy, exergy and exergo-economic analysis of solar driven supercritical carbon dioxide power and hydrogen generation cycle. Int. J. Hydrogen Energy (ISSN: 03603199) 45 (9), 5653–5667. http://dx.doi.org/10.1016/j.ijhydene.2019.06.103.

Ahmadi, M.H., Mehrpooya, M., Abbasi, S., Pourfayaz, F., Bruno, J.C., 2017. Thermo-economic analysis and multi-objective optimization of a transcritical CO 2 power cycle driven by solar energy and LNG cold recovery. Thermal Sci. Eng. Progress 4, 185–196. http://dx.doi.org/10.1016/j.tsep.2017.10.004.

Alfani, D., Binotti, M., Macchi, E., Silva, P., Astolfi, M., 2021. SCO2 power plants for waste heat recovery: design optimization and part-load operation strategies. Appl. Therm. Eng. 195, 117013. http://dx.doi.org/10.1016/j.applthermaleng.2021.117013.

Binotti, M., Astolfi, M., Campanari, S., Manzolini, G., Silva, P., 2017. Preliminary assessment of sCO2 cycles for power generation in CSP solar tower plants. Appl. Energy 204, 1007–1017. http://dx.doi.org/10.1016/j.apenergy.2017.05.121.

Calm, J., Hourahan, G., 2001. Refrigerant data summary. Eng. Syst. 18 (11), 74–88.

Crespi, F., Gavagnin, G., Sánchez, D., Martínez, G.S., 2017. Supercritical carbon dioxide cycles for power generation: A review. Appl. Energy 195, 152–183. http://dx.doi.org/10.1016/j.apenergy.2017.02.048.

Duniam, S., Veeraragavan, A., 2019. Off-design performance of the supercritical carbon dioxide recompression Brayton cycle with NDDCT cooling for concentrating solar power. Energy 187, 115992. http://dx.doi.org/10.1016/j.energy.2019.115992.

Forman, C., Muritala, I.K., Pardemann, R., Meyer, B., 2016. Estimating the global waste heat potential. Renew. Sustain. Energy Rev. 57, 1568–1579. http://dx.doi.org/10.1016/j.rser.2015.12.192.

Garapati, N., Adams, B.M., Fleming, M.R., Kuehn, T.H., Saar, M.O., 2020. Combining brine or CO2 geothermal preheating with low-temperature waste heat: A higher-efficiency hybrid geothermal power system. J. CO2 Utilization 42, 101323. http://dx.doi.org/10.1016/j.jcou.2020.101323.

Habibollahzade, A., Petersen, K.J., Aliahmadi, M., Fakhari, I., Brinkerhoff, J.R., 2022. Comparative thermoeconomic analysis of geothermal energy recovery via super/transcritical CO2 and subcritical organic Rankine cycles. Energy Convers. Manage. 251, 115008. http://dx.doi.org/10.1016/j.enconman.2021.115008.

Li, X., Huang, H., Zhao, W., 2014. A supercritical or transcritical Rankine cycle with ejector using low-grade heat. Energy Convers. Manage. 78, 551–558. http://dx.doi.org/10.1016/j.enconman.2013.11.020.

Marchionni, M., Bianchi, G., Tassou, S.A., 2018. Techno-economic assessment of Joule-Brayton cycle architectures for heat to power conversion from high-grade heat sources using CO2 in the supercritical state. Energy 148, 1140–1152. http://dx.doi.org/10.1016/j.energy.2018.02.005.

Meggitt PLC. Heatric PCHE - Performance and Efficiency.

Mirkhani, N., Amini, A., Ashjaee, M., 2017. Thermo-economic analysis of transcritical CO2 cycles with bounded and unbounded reheats in low-temperature heat recovery applications. Energy 133, 676–690. http://dx.doi.org/10.1016/j.energy.2017.05.162.

Monjurul Ehsan, M., Duniam, S., Li, J., Guan, Z., Gurgenci, H., Klimenko, A., 2020. A comprehensive thermal assessment of dry cooled supercritical CO2 power cycles. Appl. Therm. Eng. 166, 114645. http://dx.doi.org/10.1016/j.applthermaleng.2019.114645.

Nassar, A., Moroz, L., Burlaka, M., Pagur, P., Govoruschenko, Y., Designing supercritical CO2 power plants using an integrated design system. In: Proceedings of ASME 2014 Gas Turbine India Conference, 2014.

National Institute of Standards and Technology. REFPROP: NIST Reference Fluid Thermodynamic and Transport Properties Database.

Olumayegun, O., Wang, M., Kelsall, G., 2016. Closed-cycle gas turbine for power generation: A state-of-the-art review. Fuel 180, 694–717. http://dx.doi.org/10.1016/j.fuel.2016.04.074.

Pham, H.S., Alpy, N., Ferrasse, J.H., Boutin, O., Quenaut, J., Tothill, M., Haubensack, D., Saez, M., 2015. Mapping of the thermodynamic performance of the supercritical CO2 cycle and optimisation for a small modular reactor and a sodium-cooled fast reactor. Energy 87, 412–424. http://dx.doi.org/10.1016/j.energy.2015.05.022.

Sarkar, J., 2015. Review and future trends of supercritical CO2 Rankine cycle for low-grade heat conversion. Renew. Sustain. Energy Rev. 48, 434–451. http://dx.doi.org/10.1016/j.rser.2015.04.039.

Siddiqui, M.E., Almitani, K.H., 2020. Proposal and thermodynamic assessment of S-CO2 brayton cycle layout for improved heat recovery. Entropy (Basel, Switzerland) 22 (3), http://dx.doi.org/10.3390/e22030305.

Span, R., Wagner, W., 1996. A new equation of state for carbon dioxide covering the fluid region from the triple-point temperature to 1100 K at pressures up to 800 MPa. J. Phys. Chem. Ref. Data 25.6, 1509.

Steag System Technologies. EBSILON Professional for the design of power plants.

Walnum, H.T., Nekså, P., Nord, L.O., Andresen, T., 2013. Modelling and simulation of CO2 (carbon dioxide) bottoming cycles for offshore oil and gas installations at design and off-design conditions. Energy 59, 513–520. http://dx.doi.org/10.1016/j.energy.2013.06.071.

Wang, X., Dai, Y., 2016. Exergoeconomic analysis of utilizing the transcritical CO2 cycle and the ORC for a recompression supercritical CO2 cycle waste heat recovery: A comparative study. 170, 193–207. http://dx.doi.org/10.1016/j.apenergy.2016.02.112.

Wright, S., 2012. Mighty mite: a turbine that uses supercritical carbon dioxide can deliver great power from a small package.. Mech. Eng. 134, 40–43. http://dx.doi.org/10.1115/1.2012-JAN-4.

Xia, J., Wang, J., Zhou, K., Zhao, P., Dai, Y., 2018. Thermodynamic and economic analysis and multi-objective optimization of a novel transcritical CO2 Rankine cycle with an ejector driven by low grade heat source. Energy 161, 337–351. http://dx.doi.org/10.1016/j.energy.2018.07.161.